Iranian Journal of Science & Technology, Transaction B, Engineering, Vol. 30, No. B4
Printed in The Islamic Republic of Iran, 2006

UPLIFT RESPONSE OF STRIP ANCHORS IN SAND USING FEM*

J. KUMAR

Dept. of Civil Engineering, Indian Institute of Science, Bangalore-560012, India
Email: jkumar@civil.iisc.ernet.in

Abstract– The load displacement relationship of shallow rigid strip anchors embedded in sands and subjected to uplift pressures has been examined by using the finite element method. The soil medium is modeled as a linear elastic-perfect plastic material following Mohr-Coulomb failure criterion and an associated flow rule. The computed load displacement response is presented in non-dimensional form. The ultimate failure load is expressed in the form of non-dimensional uplift factor F_γ, the variation of which is plotted as a function of soil friction angle (ϕ) and the embedment ratio (λ) of the anchor. The magnitudes of F_γ, as well as the displacements of anchor at failure are found to increase with the increases in the values of the anchor embedment ratio and the angle of shearing resistance of soils. In all the cases, it was seen that even at complete collapse, the soil mass lying just vertically above the anchor remains more or less non plastic. The failure of the anchor occurs on account of the development of a thin curved plastic shear zone emerging from the bottom of the anchor and then extending up to the ground surface.

Keywords– Anchors, failure, finite elements, foundations, sands, uplift

1. INTRODUCTION

The problem of the determination of the pullout resistance of anchors is often encountered in the foundations of structures such as transmission towers, drydocks and buried pipe lines under water. This problem has been tackled by various investigators in a number of different ways. Meyerhof and Adams [1] have made use of the passive earth pressure coefficients of Caquot and Kerisel [2] in developing the theory for the vertical uplift capacity of foundations. Vesic [3] has utilized the concept of expansion of cylindrical and spherical cavities in the soil mass in finding the pullout resistance. For determining the pullout capacity of anchors, Murray and Geddes [4] and Kumar [5, 6] have used the upper bound theorem of limit analysis based on the assumption of an associated flow rule material. The upper bound limit analysis solutions, with the simple assumption of linear rupture surfaces, compare favorably with the limit equilibrium approach of Meyerhof and Adams [1]. Rowe and Davis [7] have employed the elasto-plastic finite element method in computing the pullout resistance of horizontal and vertical anchors. In their analysis the effects of anchor roughness, initial stress state and the dilatancy angle of the soil on the uplift resistance were also examined. It was shown that the vertical uplift capacity of horizontal anchors remains mostly unaffected with the changes in the initial stress state and the anchor roughness. An increase in the dilatancy angle was shown to result in a considerable increase in the uplift resistance. However, the predictions of the uplift resistance in sands from Rowe and Davis's finite element computations have been found to be much greater as compared to the simple upper bound limit analysis solutions [4, 5] on the basis of linear rupture surfaces. Subba Rao and Kumar [8] have solved the anchor problem by using the Sokolovoski's method of characteristics and on the assumption of composite logarithmic spiral failure

*Received by the editors May 11, 2004; final revised form November 23, 2005.
**Corresponding author

surface. The uplift resistance from this approach has been found to be generally conservative as compared to most of the existing theories. A good review of the literature on the determination of the uplift resistance of soil mass is provided by Sutherland [9]. In the present article, the vertical uplift resistance of strip anchors has been obtained by using the elasto-plastic finite element method. The developments of the plastic zones around the anchor were also examined. The anchor itself has been treated as a completely rigid body, whereas the soil material has been modeled as a linear elastic-perfectly plastic material following Mohr-Coulomb failure criterion and an associated flow rule. The effect of the embedment ratios of the anchors and the friction angle of the soil mass on the results has been studied in detail. The results have been compared with those reported in the literature.

2. DEFINITION OF THE PROBLEM

Given a strip anchor of width b located at a depth d from the horizontal ground surface as shown in Fig. 1. The anchor is perfectly rigid and is buried in a cohesionless soil medium. The thickness of the plate is negligible as compared to its width. The plate is assumed to be fully bonded to the surrounding soil mass, and no separation was considered inbetween the plate and the soil mass. It is required to assess the load deformation response of the anchor till the ultimate pullout failure, and then to establish the magnitudes of the failure load. In the given analysis, the value of b was kept equal to 0.5 m, and the embedment ratio (λ = d/b) was varied between 1 and 7. The values of the elastic modulus (E) and the Poisson ratio (ν) of the material were taken equal to 20,000 kPa and 0.3 respectively. The friction angle (ϕ) of the soil mass was varied between 30 and 45 degrees. The soil unit weight (γ) was kept equal to 20 kN/m^3. It should be mentioned that all the results have been presented in non-dimensional fashion and the chosen values of E and γ do not affect the answer.

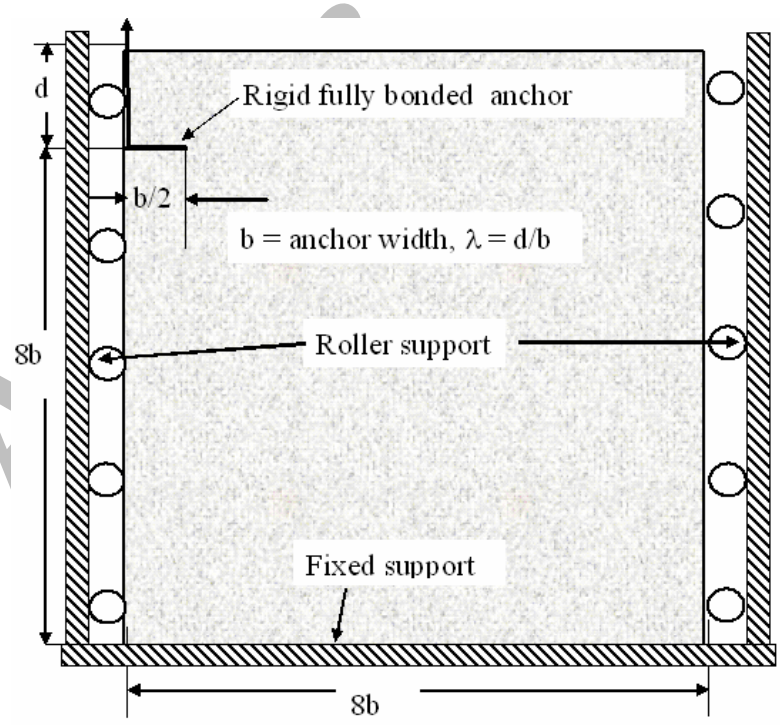

Fig. 1. Boundary conditions and the chosen FE domain

3. CONSTITUTIVE MODEL

It was assumed that the soil medium is linearly elastic perfect plastic material following the Mohr-Coulomb failure criterion and an associated flow rule. The incremental stresses {dσ} were related to the

total incremental strains {dε} via the elasto-plastic stiffness matrix $[D^{ep}]$; the text books of Chen [10] and Chen and Mizuno [11] can be referred to for the derivations:
For the present plane strain problem

$$[D^{ep}]_{4\times4} = [D^{e}]_{4\times4} - \frac{[D^{e}]_{4\times4}\left[\frac{\partial F}{\partial \sigma}\right]_{4\times1}\left[\left(\frac{\partial F}{\partial \sigma}\right)^{T}\right]_{1\times4}[D^{e}]_{4\times4}}{\left[\left(\frac{\partial F}{\partial \sigma}\right)^{T}\right]_{1\times4}[D^{e}]_{4\times4}\left[\frac{\partial F}{\partial \sigma}\right]_{4\times1}} \tag{1}$$

where, F is the yield function

$$F = \frac{I_1}{3}\sin\phi + \sqrt{J_2}\left(\cos\alpha - \frac{\sin\alpha\sin\phi}{\sqrt{3}}\right) - c\cos\phi \tag{2}$$

$$\left[\left(\frac{\partial F}{\partial \sigma}\right)^{T}\right]_{1\times4} = \left[\frac{\partial F}{\partial \sigma_x} \quad \frac{\partial F}{\partial \sigma_y} \quad \frac{\partial F}{\partial \sigma_z} \quad \frac{\partial F}{\partial \tau_{xy}}\right] \tag{3.1}$$

$$J_2 = \left(\frac{(s_x^2 + s_y^2 + s_z^2)}{2} + \tau_{xy}^2 + \tau_{yz}^2 + \tau_{zx}^2\right) \tag{3.2}$$

$$J_3 = s_x s_y s_z + 2\tau_{xy}\tau_{yz}\tau_{zx} - s_x\tau_{yz}^2 - s_y\tau_{xz}^2 - s_z\tau_{xy}^2 \tag{3.3}$$

$$\alpha = \frac{1}{3}\sin^{-1}\left(-\frac{3J_3\sqrt{3}}{2J_2^{3/2}}\right) \tag{3.4}$$

where $I_1 = \sigma_x + \sigma_y + \sigma_z$; $s_x = \sigma_x - I_1/3$; $s_y = \sigma_y - I_1/3$; $s_z = \sigma_z - I_1/3$, and $[D^e]_{4x4}$ is the elastic stiffness matrix for the plane strain case.

The yield function F can also be related to the major and minor principal stresses $(\sigma_1 \& \sigma_3)$ with the equation

$$F = \frac{(\sigma_1 - \sigma_3)}{2} - \frac{(\sigma_1 + \sigma_3)}{2}\sin\phi - c\cos\phi \tag{4}$$

The details of the formulation and the associated program are presented in Kumar [12].

4. FINITE ELEMENT MESH AND BOUNDARY CONDITIONS

It was assumed that the effect of the loading of the anchor is negligible at horizontal and vertical distances equal to 8b from the center of the anchor respectively. On account of the symmetry of the anchor about its axis, only one half of the soil domain enclosed within the extreme vertical boundaries was considered. For the chosen soil domain, along both the vertical boundaries (one of which forms the axis of the anchor), the displacement constraint only in the horizontal direction was provided. Along the horizontal boundary line below the anchor, displacement constraints both in horizontal and vertical directions were imposed. The boundary conditions for the chosen soil domain are shown in Fig. 1. Along the periphery of the anchor, uniform displacement increments of the anchor were given in the vertical direction and no displacement constraint was provided in the horizontal direction. The anchor plate was assumed to be fully bonded with the soil mass and no separation of the soil material from the periphery of the anchor was allowed to occur

during the course of the analysis. The soil mass as enclosed within the defined boundaries of the domain was discretized into a mesh of six noded linear strain triangular elements. The finite element mesh was generated in such a fashion that the elements approaching the periphery of the anchor become gradually smaller in size. The obtained finite element mesh for two different embedment ratios is shown in Figs. 2a and 3a. The number of elements vary between 1398 and 1572, and the number of nodes chosen between 723 and 811.

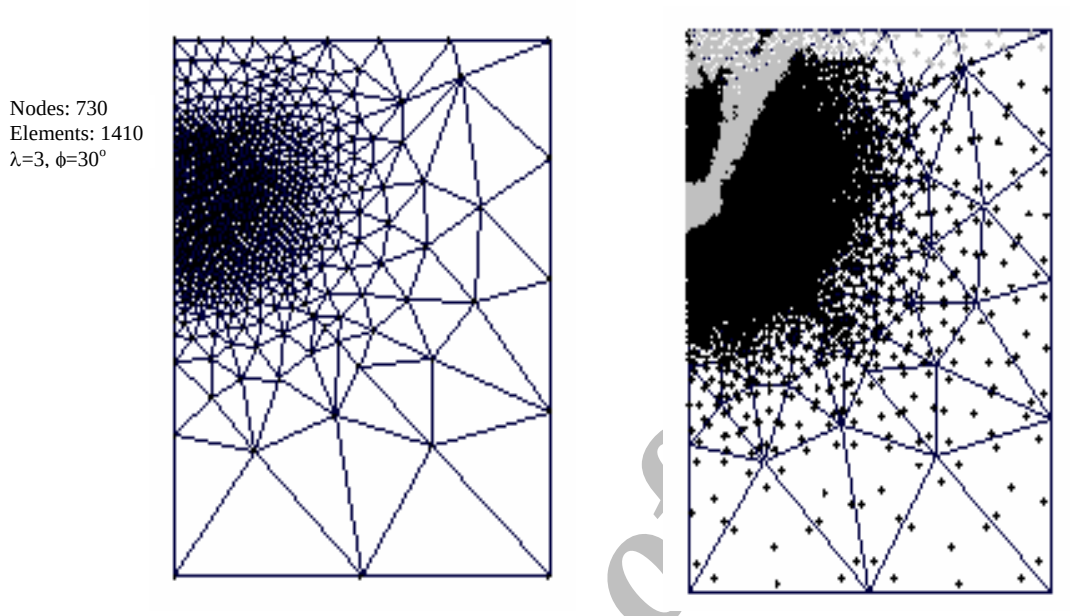

(a) (b)

Fig. 2. FE mesh and plastic zone pattern for $\lambda = 3$ and $\phi = 30^o$

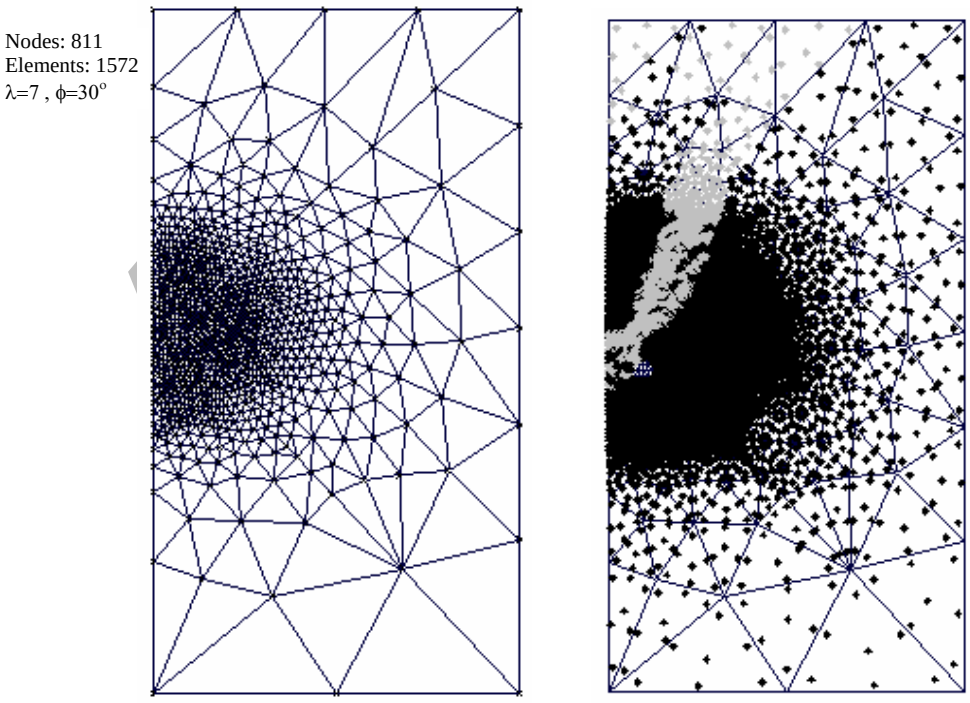

(a) (b)

Fig. 3. FE mesh and plastic zone pattern for $\lambda = 7$ and $\phi = 30^o$

5. ANALYSIS

Before launching the elasto-plastic FE analysis, in situ stresses everywhere were fixed by assuming K_o condition in the soil mass, and the magnitude of earth pressure coefficient K_o was kept equal to 1.0. Since it is known that the variation in K_o does not affect the magnitude of the failure load [11, 13], its effect on the pullout resistance of anchors was not, therefore, investigated in the present paper. After establishing the in-situ stresses from the K_o condition, the finite element analysis was then started by imposing equal vertical upward displacement increments everywhere along the periphery of the anchor. Each increment of the displacement was further subdivided into 100 small increments. During each small displacement increment, the modified Newton-Raphson iterative technique was used to account for the non-linearity due to the elasto-plastic stiffness matrix. A displacement criterion was used to check for the convergence. The convergence was said to be achieved when the ratio of the square root of the sum of displacements in the current iteration to the square root of the sum of the total displacements up to the current iteration was equal to or less than 1%. It was seen that 20-30 iterations were sufficient enough to achieve the convergence in all the cases. Displacement increments of the anchor were continued till the complete failure of the anchor was observed. After each small increment of displacements, the co-ordinates of all the nodes were continuously updated by knowing the computed increments of nodal displacements. For a given displacement, the uplift load P_u per unit length of the anchor plate was obtained by adding all the vertical reactions along the nodes of the anchor plate. The average vertical uplift pressure p_u was defined as P_u/b. The magnitude of p_u at failure ($p_{u,ult}$) was expressed in the form of uplift factor F_γ as defined below

$$p_{u,ult} = \gamma d F_\gamma \tag{5}$$

6. RESULTS

The obtained uplift pressure displacement response was related to the non dimensional way; the uplift pressure was expressed as $p_u/(\gamma d)$, and the uplift displacement (δ) of the anchor was presented in the form of dimensionless parameter $E\delta/(\gamma bd)$. The non-dimensional uplift pressure- displacement relationships in all the cases are shown in Figs. 4-7. It can be seen that in all the cases, initially, the pressure displacement response remains linear, and then the slope (stiffness) of the plotted curves decreases continuously till the complete failure occurs. The magnitude of the failure load, the failure displacement and the initial stiffness of the load-displacement curves become larger for higher values of λ and ϕ. From the obtained pressure versus displacement relationship, the failure loads were determined in all the cases. From the known magnitude of failure loads, the uplift factor F_γ was then determined using Eq. (5). The variation of F_γ with λ and ϕ is shown in Fig. 8. It can be seen that the uplift factor increases continuously with the increases in ϕ and λ. The effect of ϕ on the pullout resistance of anchors becomes more appreciable for higher embedment ratios. In addition to examining the pressure displacement relationships of the anchors, the failure status of all the elements at their integrating points was also noticed. It was seen that even at complete collapse, the soil mass lying just above the anchor remains mostly non-plastic. The collapse of the anchors in all the cases occurs on account of the development of a thin curved plastic (shear) zone which generates from the bottom of the anchor and then extends up to the ground surface. The obtained patterns of the plastic zones for two different cases viz. (i) $\phi=30^o$ and $\lambda=3$; (ii) $\phi=30^o$ and $\lambda=7$, are indicated in Figs. 2b and 3b; the colour of the integration points in these figures was shown to be light for the points where the failure was noticed. It can be seen that the extent of failure surface at the ground increases with the increase in the values of λ and ϕ.

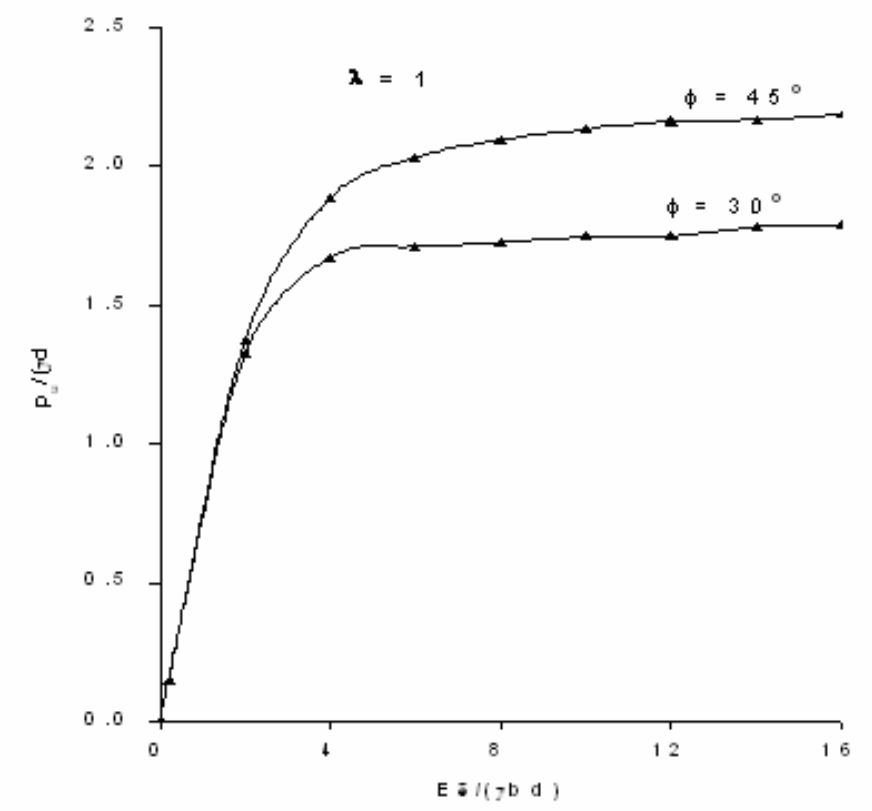

Fig. 4. Non-dimensional uplift pressure-displacement response for λ =1

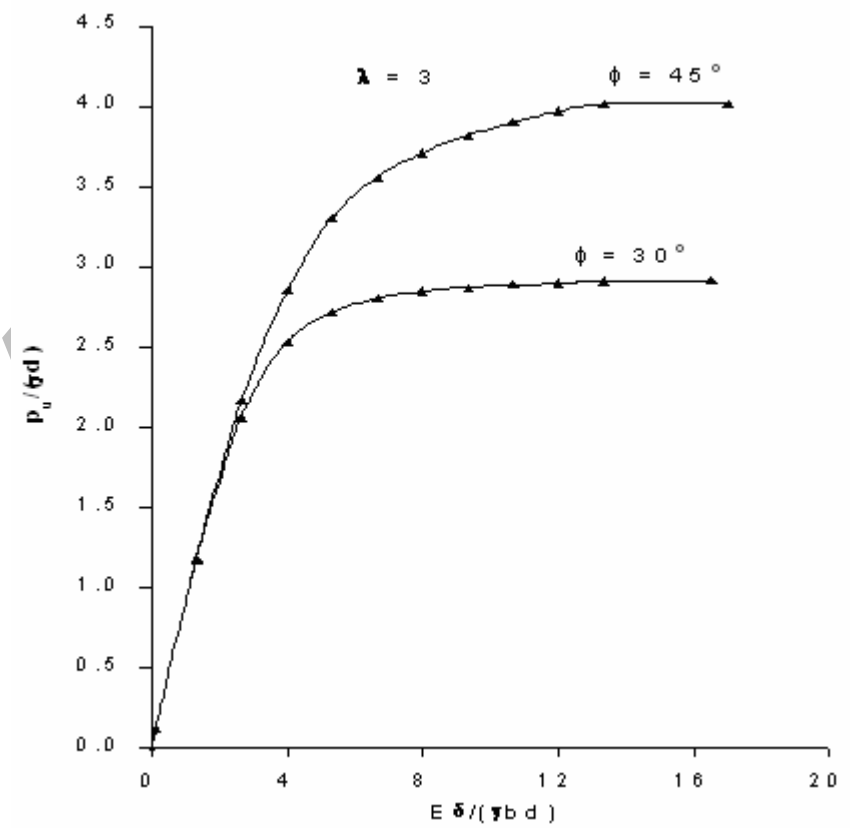

Fig. 5. Non-dimensional uplift pressure-displacement response for λ =3

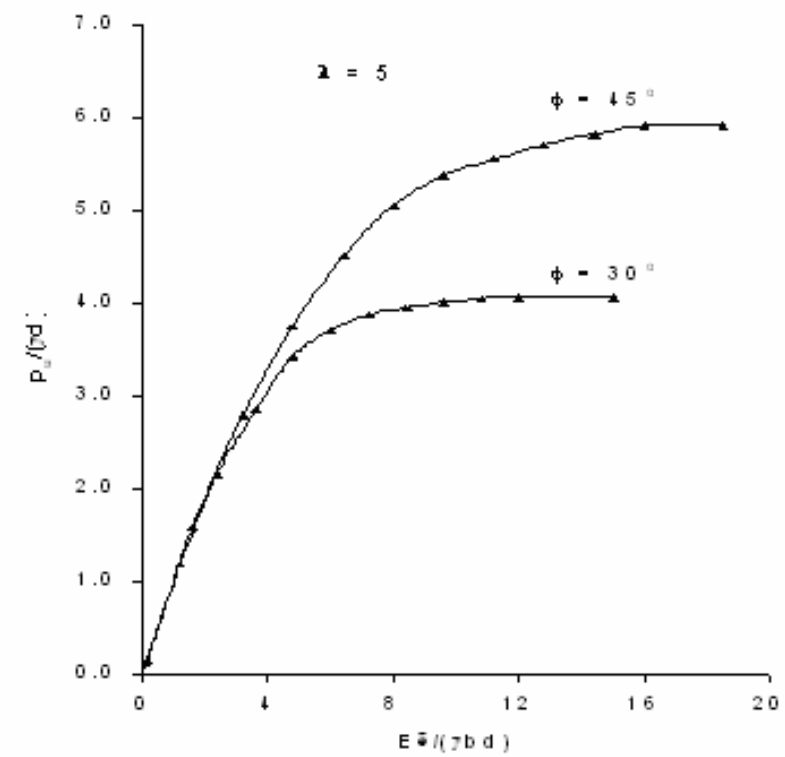

Fig. 6. Non-dimensional uplift pressure-displacement response for λ =5

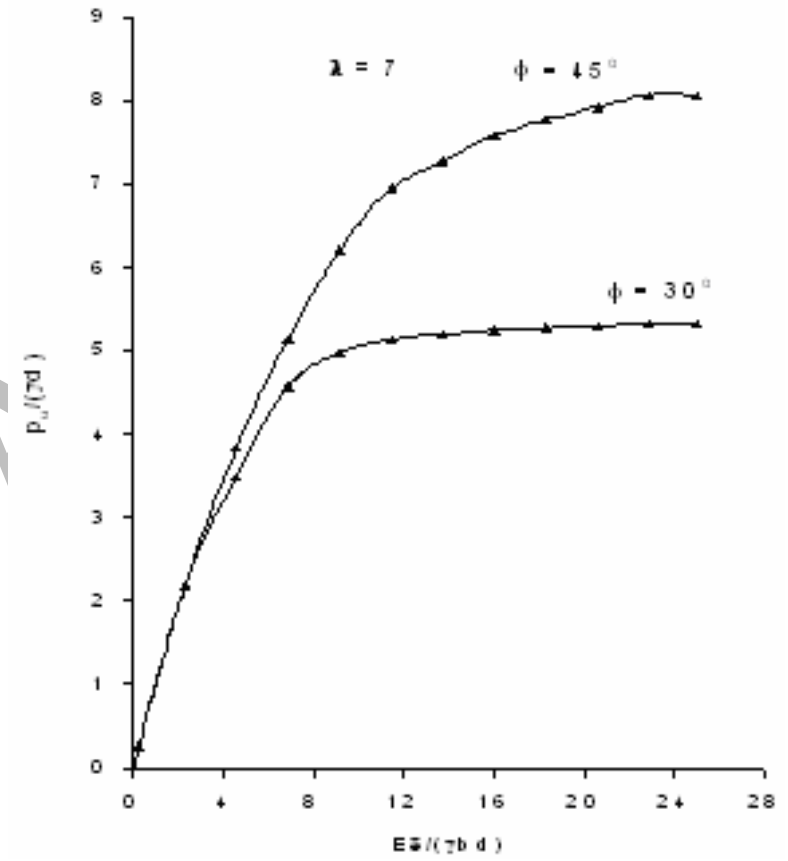

Fig. 7. Non-dimensional uplift pressure-displacement response for λ =7

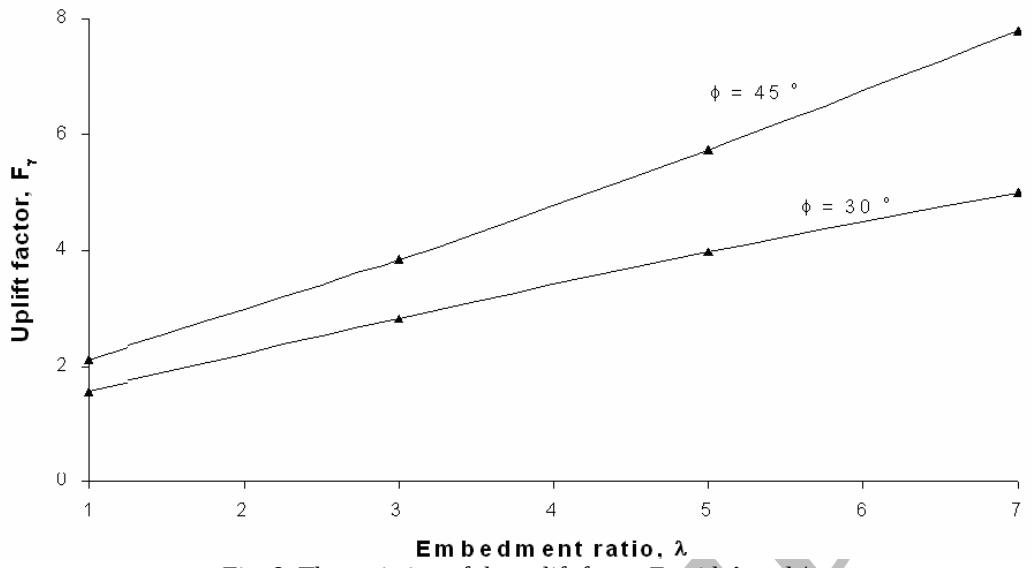

Fig. 8. The variation of the uplift factor F_γ with λ and ϕ

7. COMPARISONS

a) With the available theories

The obtained values of the uplift factor, F_γ, from the present FE analysis were compared with the FE analysis of Rowe and Davis [7] using an associated flow rule, (dilatancy angle, $\psi = \phi$), the limit equilibrium study of Meyerhof and Adams [1], the method of stress characteristic solution of Subba Rao and Kumar [8] and the upper bound limit analysis solution of Murray and Geddes [4]. The obtained comparison for ϕ=30^o and 45^o is shown in Figs. 9 and 10. It can be seen that the present FE results on the anchors compare most favorably with the theories of Meyerhof and Adams [1] and Murray and Geddes [4]. The theory of Rowe and Davis [7] provides the maximum uplift resistance. On the other hand, the analysis of Subba Rao and Kumar [8] on the basis of the method of characteristics was seen to be the most conservative. It should be mentioned that the results from the method of characteristics often matches well with the finite element results for a material with an associative flow rule. The results from the method of characteristics always provides the lower bound solution, that is, the magnitude of the true failure load will be either greater or at least equal to the ultimate failure load determined from the method of characteristics. The present comparison is in accordance with this observation. However, the greater difference between the two is due to the fact that the analysis of Subba Rao and Kumar [8] is based upon the additional assumption of the logarithmic spiral shape of the failure surface.

b) With the experimental data

For a strip anchor plate with a width of 51mm, Rowe and Davis [7] presented experimental results for anchors buried in sand. Two different values of unit weight, namely 14.90 kN/m^3 and 15.27 kN/m^3 of sand mass were used in their experiments. The corresponding peak angles of friction were found to be 35.2^o and 36.6^o, respectively. The angles of diltation (ψ) were also determined by Rowe and Davis [7] and the corresponding values of ψ were seen to be 4^o and 10^o, respectively. The values of the average ultimate uplift pressures obtained from these experiments were compared with the results from the present analysis using an associative flow rule. The comparison of the results is provided in Table 1 for different values of λ. It can be seen that the finite element results from the present analysis compare reasonably well with the experimental results of Rowe and Davis [7]. As compared to the experimental results, the theory provides higher values of the pullout resistance. It should be mentioned that the theoretical values are on the basis

of an associative flow, and therefore, it was expected that the present analysis will yield greater pullout resistance as compared to the experimental observation where the value of ψ is much smaller than ϕ.

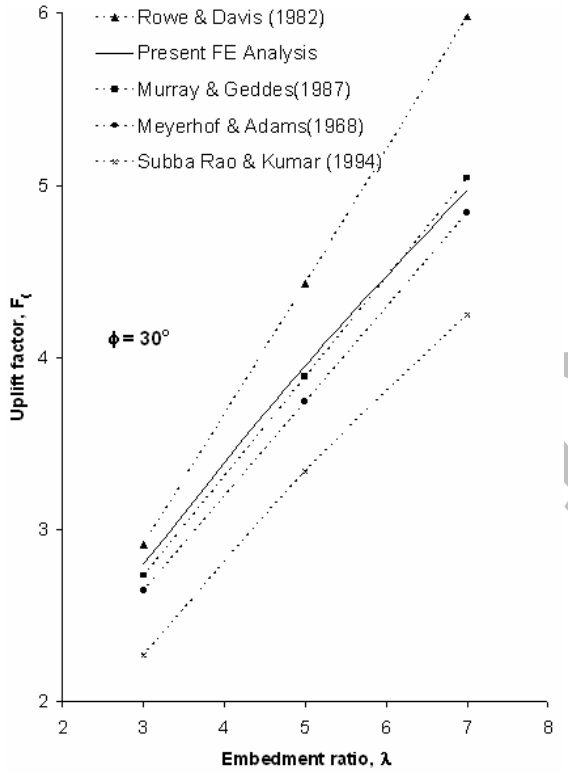

Fig. 9. Comparison of the uplift factor F_γ for $\phi = 30^o$

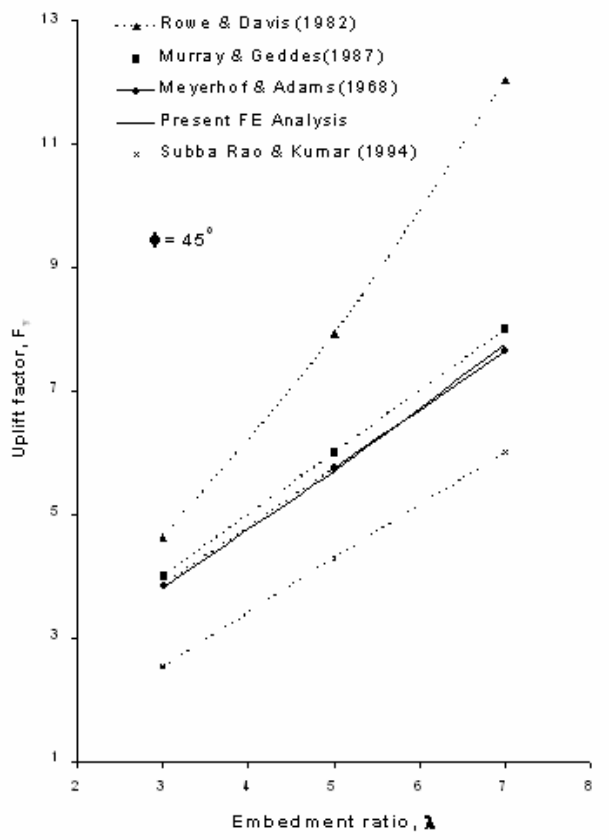

Fig. 10. Comparison of the uplift factor F_γ for $\phi = 45^o$

Similar to the present findings, the experimental observations of Matsuo [14, 15] and the present analysis also indicate the development of the curved shear zones. It should be mentioned that the findings of Matsuo are for a circular shape of the anchor. Due to the circular shape of the anchor, the pullout resistance obtained by Matsuo could not be compared with the present analysis.

Table 1. Comparison of the experimental results of Rowe and Davis [7] with the present analysis for strip anchors in sand

λ	Average ultimate uplift pressure (p_u) in kPa for strip anchor with width (b) = 51 mm			
	γ = 14.90 kN/m^3 ϕ = 35.2^o, ψ = 4^o		γ = 15.27 kN/m^3 ϕ = 36.6^o , ψ = 10^o	
	Experimental data of Rowe and Davis (1982b)	Present FE analysis for ϕ=35.2^o with $\psi = \phi$	Experimental data of Rowe and Davis [7]	Present FE analysis for ϕ=36.6^o with $\psi = \phi$
1	1.11	1.35	-	1.42
2	2.99	3.74	-	3.94
3	5.74	7.20	6.03	7.60
4	9.09	11.74	-	12.43
5	14.45	17.35	15.65	18.43
6	20.45	24.00	-	25.60
7	26.45	31.65	-	33.88

8. DISCUSSION

(i) The soil mass is assumed to obey an associated flow rule. It is known that an increase in volume during shear predicted on this assumption is usually much greater than that usually observed in most of the soils. It is also understood that the failure load for a non-associated flow rule material will usually be smaller than that for the associated flow rule material [16, 17]. Therefore, the true failure load will generally be lower than that presented in this paper. In other words, the answer provided in this paper will not be conservative. For a non-associated flow rule, the modified value of ϕ can be used to predict the uplift resistance as per the recommendation of Drescher and Detournay [17] based on the given value of dilatancy angle (ψ).

$$\phi^* = \tan^{-1}(\xi \tan\phi) \tag{6.1}$$

$$\xi = \frac{cos\psi cos\phi}{1 - \sin\psi \sin\phi} \tag{6.2}$$

where ϕ* is the modified value of ϕ to account for the effect of ψ.

(ii) It may be noted that the ultimate pullout resistance computed from the analysis of Rowe and Davis [7] always remains greater than that of the present values. In both the analyses, the size of the problem domain and the associative boundary conditions were kept exactly the same. In the analysis of Rowe and Davis [7], it has been assumed that upon the subjection of the uplift pressure, the underlying soil mass at failure gets separated from the base of the anchor plate. On the other hand, in the present analysis, no such separation of the soil mass from under the base of the anchor plate was allowed and the soil was assumed to always remain fully bonded with the anchor plate. As a result, the vertical uplift soil pressure acting on the base of the anchor plate will help in the uplift movement of the anchor and therefore, the uplift resistance becomes lower as compared to the analysis of Rowe and Davis [7]. In the analysis of Rowe and Davis [7], the vertical uplift pressure acting underneath the anchor plate during yielding becomes equal to zero on account of separation. It should be mentioned initially that no separation occurs and the initial stiffness of the load-displacement curves of Rowe and Davis [7] becomes exactly the same as that of the

present analysis. For Poisson ratio (ν) = 0.3, the values of the initial stiffness for different values of λ were compared with those obtained by Rowe and Davis [7]; it should be mentioned that the initial stiffness of the load-deformation curves does not depend on the value of ϕ. The comparison is shown in Fig. 11. It can be seen that the results of Rowe and Davis are exactly the same as those obtained in the present study.

(iii) It should be noted that for a given value of λ, the magnitude of $E\delta/(\gamma bd)$ required to cause the ultimate failure of the anchor plate increases only marginally with an increase in the magnitude of friction angle ϕ. In order to have the same value of $E\delta/(\gamma bd)$, the value of δ will decrease continuously with an increase in the value of E. It is known from the experiments that the amount of displacement required to attain failure is usually smaller for a dense sand as compared to loose sand [1]. It needs to be mentioned that for a dense sand, the value of the elastic modulus will be much greater than that of the loose sand. Therefore, in order to attain the same value of $E\delta/(\gamma bd)$, the displacement required to reach failure will become much smaller in the case of anchors buried in dense sand.

(iv) In the present study, it has been assumed that the soil mass before reaching failure always remains linearly elastic. The effect of non-linearity of the pre-failure stress-strain relationship of the soil mass has not been explored in this paper.

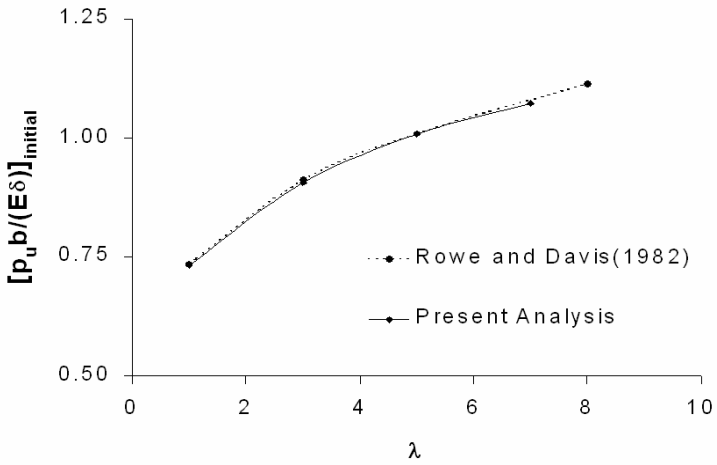

Fig. 11. Comparison of the initial stiffness of the load-displacement curves in Figs. 4-7.

9. CONCLUSIONS

On the basis of elasto-plastic finite element study, the force displacement response of rigid anchors placed in sands and subjected to uplift pull is examined. The failure loads have been obtained in the form of uplift factor F_γ. The magnitude of the uplift factor increases with the increases in the values of the embedment ratio(λ) of the anchor and the friction angle (ϕ) of the soil. The influence of the friction angle on the pullout resistance is found to be more considerable at higher embedment ratios. In all the cases, it has been noticed that even at complete collapse, the soil mass lying above the anchor remains more or less non-plastic. The collapse of the anchors occurs on account of the development of a thin curved plastic shear zone emerging from the bottom of the anchor and then terminating at the ground surface.

REFERENCES

1. Meyerhof, G. G. & Adams, S. I. (1968). The ultimate uplift capacity of foundations. *Canadian Geotechnical Journal*, *5*(4), 225-244.
2. Caquot, A. & Kerisel, L. (1949). Traite de mecanique des sols, *Gauthier Villars*, Paris, France.
3. Vesic, A. S. (1971). Breakout resistance of objects embedded in a ocean bottom. *J. Soil Mech. Fdns. Div., ASCE, 97*, 1183-1205.

4. Murray, E. J. & Geddes, J. D. (1987). Uplift of anchor plates in sand. *Journal of Geotech. Engrg., ASCE*, *113*(3), 202-215.
5. Kumar, J. (1997). Upper bound solution for pullout capacity of anchors on sandy slopes. *Int. Jour. Numer. Analyt. Meth. Geomech*., USA, *21*, 477-484.
6. Kumar, J. (1999). Kinematic slices approach for uplift analysis of strip foundations, *Int. Jour. Numer. Analyt. Meth. Geomech*., *23*, 1159-1170.
7. Rowe, R. K. & Davis, E. H. (1982). The behaviour of anchor plates in sand, *Geotechnique*, *32*(1), 25-41.
8. Subba Rao, K. S. & Kumar, J. (1994). Vertical uplift capacity of horizontal anchors, *Journal of Geotech. Engrg*., ASCE, USA, *120*(7), 1134-47.
9. Sutherland, H. B. (1988). Uplift resistance of soils, 28th Rankine lecture. *Geotechnique, 38*(4), 493-516.
10. Chen, W. F. (1975). Limit analysis and soil plasicity, *Elsevier*, NewYork,.
11. Chen, W. F. & Mizuno, E. (1990). Non linear analysis in soil mechanics, *Elsevier*, NewYork.
12. Kumar, J. (2002). Uplift response of buried pipes using FEM, *Indian Geotechnical Journal*, *32*(2), 146-160.
13. Griffiths, D. V. (1982). Computation of bearing capacity factors using finite elements. *Geotechnique, 32*(3), 195-202.
14. Matsuo, M. (1967). Study on the pullout resistance of footing (I). *Soils and Foundations*, Japan, *7*(4), 1-37.
15. Matsuo, M. (1968). Study on the pullout resistance of footing (II), *Soils and Foundations*, Japan, *8*(1), 18-48.
16. Zienkiewicz, O. C., Humpheson, C. & Lewis, R. W. (1975). Associated and non-associated visco-plasticity and plasticity in soil mechanics, *Geotechnique*, *25*, 671-89.
17. Drescher, A. & Detournay, E. (1993). Limit load in translational failure mechanisms for associated and non-associated materials, *Geotechnique*, *43*(3), 443-456.